

## INVESTIGATION OF EFFECTS OF SINGLE OVERLOAD/UNDERLOAD ON CRACK OPENING LOAD VALUES OF 350WT STEEL USING FINITE ELEMENT METHOD

M. H. Gozin and M. Aghaie-Khafri

K.N. Toosi University of Technology, Tehran, Iran

### ABSTRACT

There have been numerous efforts to account for the crack growth retardation phenomena. Among them the plasticity-induced crack closure (PICC) concept has been supported by a number of investigators. In present study, effects of single overload and single overload following by underload on crack growth retardation of center-cracked specimen of 350WT steel is studied. A two-dimensional finite element model was built using four node plane stress elements. Mesh refinement procedure used to approach predefined convergence. Fatigue crack growth was modeled by repeatedly applying loading-unloading cycles and advancing crack front. Mesh refinement studies indicate that at least four element in reversed plastic zone are needed to conduct opening load convergence. Under constant amplitude loading conditions, the crack must be advanced completely through the initial forward plastic zone to form a stabilized plastic wake. Finite element simulation of single overload illustrates that crack opening load values decreases just after applying single overload and then increases to its maximum value.

**Keywords:** Finite Element Methods, Fatigue, Crack Closure, Opening Load Value, Single Overload.

### 1. INTRODUCTION

Many structural materials are subjected to variable-amplitude fatigue loading rather than constant amplitude fatigue loading. Sudden changes in the cyclic loading patterns during fatigue deformation could give rise to complicated plastic zones in the vicinity of the crack tip and result in a considerable acceleration or retardation in the crack growth rate owing to these load interaction effects. Therefore, a fundamental understanding of the overload or underload effects and damage mechanisms will help enhance the lifetime prediction capabilities and improve the damage tolerance design for critical application exposed to random fatigue loadings. There have been numerous efforts to account for the crack growth retardation phenomena, which include both experimental studies [1–6] and computer simulation studies [7–10]. Among them, the plasticity-induced crack closure concept suggested by Elber [11] has been supported by many investigations [7–10, 12-19].

PICC occurs due to that the yielded material left in the wake of a crack tip as it propagates through plastic zones during the fatigue process [20]. The plastic wake enables the crack to close before minimum load is reached. Elber showed that the stress intensity factor at the crack tip does not change while the crack is closed. Effective stress intensity factor is calculated as following:

$$\Delta K_{eff} = K_{max} - K_{OP} \quad (1)$$

Where  $k_{max}$  and  $k_o$  are maximum and opening stress intensity factors. Crack growth rate relates to effective stress intensity;

$$\frac{da}{dN} = g(\Delta K_{eff}) \quad (2)$$

A number of researchers have simulated plasticity-induced closure using finite element analyses. McClung and Sehitoglu [16] and Solanki et al. [14] have provided critical overviews of this work. The basic algorithm employed by most researchers is the same. An elastic–plastic finite element model is built with a suitably refined mesh, and time-dependent remote tractions are applied to simulate cyclic loading. The crack tip node is released during each cycle, advancing the crack one element length and allowing a plastic wake to incrementally form. Crack closure is predicted by monitoring the contact between crack faces. This process is repeated until the crack opening stress values have stabilized.

### 2. MATERIAL, SPECIMEN AND TESTS

#### 2.1. Material

The starting material was used by Taheri's

experiments [5] and Rushton and Taheri [3] was 350WT steel. The chemical composition and mechanical properties of which are listed in Table 1 and 2, respectively. The as-received materials were sized to 300×150×5 mm with a 20 mm crack in longitudinal orientation. Sample preparation and fatigue testing were conducted in accordance with ASTM E647. All the samples were sufficiently thin that crack measurements were only required on one surface of the specimen.

## 2.2. Taheri experiment

Taheri et al. [5] conducted an experimental fatigue program consisting of constant and semi-random (variable) amplitude cyclic loadings using the center-cracked specimen shown in Fig. 1. The degree of fatigue crack growth retardation resulting from tensile overloads interspersed within a constant amplitude loading sequence was studied by Taheri et al. [5].

## 2.3. Rushton and Taheri Experiment

Tensile overload immediately followed by a compressive underload and the resulted reduction in fatigue crack growth retardation was considered by Rushton and Taheri [3]. The constant amplitude portion of the loading sequence involves cycling at maximum stress of 120 MPa. Two stress ratios namely  $R=0.1$  and  $0.3$  were considered during the tests. At each stress ratio, three levels of overload ratio ( $OLR=1.20, 1.50, \text{ and } 1.67$ ) were applied.

Table 1: chemical composition of 350WT Steel

| Specimen % | Chemical   | 350WT     |
|------------|------------|-----------|
| 0.075      | carbon     | 0.22(max) |
| 0.034      | chromium   | N/A       |
| 0.016      | cobalt     | N/A       |
| 0.01       | copper     | N/A       |
| 1.25       | manganese  | .08-1.5   |
| 0.006      | molybdenum | N/A       |
| 0.3        | niobium    | N/A       |
| 0.008      | nickel     | N/A       |
| 0.009      | phosphorus | .03(max.) |
| 0.23       | silicon    | .15-.4    |
| 0.052      | vanadium   | N/A       |
| 0.004      | sulfur     | .03(max.) |

Table2: Material properties of 350 WT Steel

| Material property                 | Value   |
|-----------------------------------|---------|
| Yield strength, $\sigma_{yld}$    | 450 MPa |
| Ultimate strength, $\sigma_{ult}$ | 524 MPa |
| Reduction in area, RA             | 71%     |
| Modulus of elasticity, E          | 205 GPa |
| Poisson's ratio, $\nu$            | 0.30    |

## 3. FINITE ELEMENT SIMULATION

Finite element analysis was used to simulate the fatigue crack growth in center-cracked 350WT steel specimens. The commercial finite element program ABAQUS 6.8.1 was employed. To simulate the stress-strain behavior of the material, elastic-perfectly plastic model was chosen and the Von-Mises yield criterion was implemented. A two-dimensional mesh was built using four nodes plane stress elements. Concerning specimen symmetry one quarter of the sample was modeled. Mesh refinement procedure was used around the crack tip region to approach predefined convergence. The final mesh consisted of 29778 elements and 29453 nodes (figure 1). The elements along the direction of crack advance had a length of 0.05 mm. The constant amplitude loading sequence was modeled by applying 120 MPa stress in each cycle. Considering simulation of the overload/underload, uniform stresses were applied and removed in each cycle. The magnitude of the conducted stresses was 144 MPa, 180 MPa and 200 MPa corresponding to overload ratios of 1.2, 1.5 and 1.67, respectively. Fatigue crack growth was modeled by repeatedly applying two loading-unloading cycles then advancing crack front. The model was incrementally approached to the maximum load then unloaded to minimum load. At minimum load the crack tip node was released and the crack advanced one element length per load cycle. During each increment of loading, the displacement of the first node adjacent to the crack tip was monitored. Following each increment, if the nodal displacement becomes positive, the crack assumes to be open. Computation of the crack opening stress,  $S_{op}$ , and the corresponding stress intensity factor,  $K_{op}$ , is the main goal of this stage.

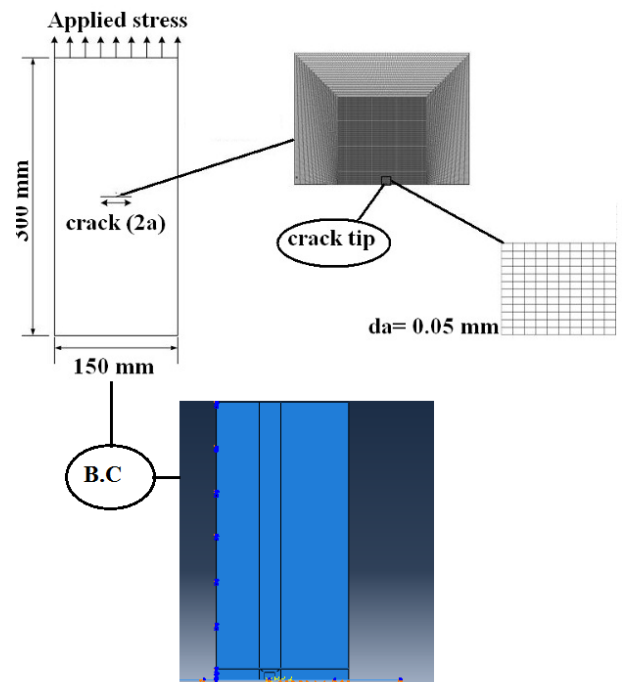


Fig 1. Finite element model

### 3.1 Mesh Refinement

To study the effects of mesh refinement, crack growth analyses were performed after reducing the element size consecutively by a factor of 1/2 or 1/3. Each time a more refined mesh was used, the same amount of total crack growth was modeled. This naturally led to an extremely refined mesh and the use of many load cycles. For perspective, the element sizes reported in the literature and normalized are shown in table 2. The variation in the number of elements in the plastic zones as the mesh refinement is illustrated in figure 2. It is clear from the figure that the number of elements along the crack plane in the reversed plastic zone is significantly lower than in the forward plastic zone. Thus, a large refinement level is required to accurately determine the reversed plastic zone.

Table 3: Distribution of mesh refinement levels

| author         | year | Normalized element size(L/rp) |
|----------------|------|-------------------------------|
| Ogura et al.   | 1977 | 0.7                           |
| Kfouri         | 1983 | 0.4                           |
| Fleck          | 1988 | 0.3                           |
| Ashburgh       | 1997 | 0.25                          |
| Bloum et al.   | 1985 | 0.1                           |
| Solanki et al. | 2003 | 0.03                          |
| Current study  | 2011 | 0.025                         |

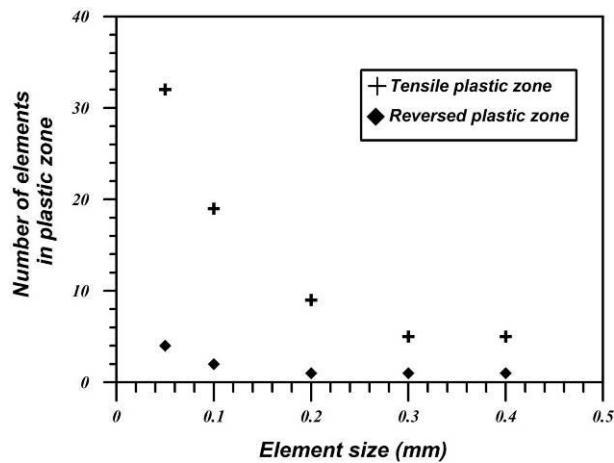


Fig 2. Variation in plastic zone size with mesh refinement

### 3.2 Crack Growth Stabilization

Under constant amplitude loading conditions, the crack must be advanced completely through the initial forward plastic zone to form a stabilized plastic wake. Fig. 3 illustrates that crack should be advanced at least eight steps before plastic wake forms and crack opening load stabilized. Therefore, to approach more exact results before any step of overload (overload/underload), thirty steps of crack growth applied.

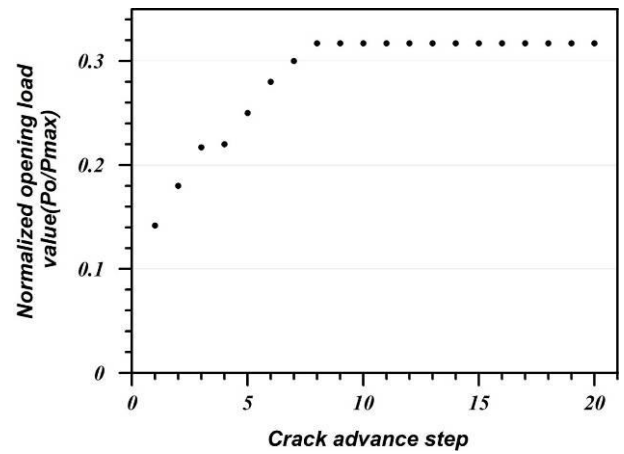


Fig 3. Crack opening load transient behavior (no overloads)

## 5. RESULTS

After conducting appropriate mesh refinement and adequate number of steps before applying overload/undeload, effect of single overload on crack opening value studied. As shown in Fig4, three levels of OLR=1.2, 1.5 and 1.67 were applied and crack opening load calculated using first node before crack tip displacement. For all overload ratios there is an opening load drop just after applying single overload. Continuously advancing the crack, opening load rises to its maximum and then slowly reduces to constant value equals to no overload opening load. It is clear from the figure that higher OLR ratios results in higher opening loads and needs more steps of crack growing before converging to constant value. Maximum value of opening load is 0.7 of maximum load and contributes to OLR=1.67. It means that plastic wakes due higher overload ratios are bigger and stay much longer after crack grows. Effect of underloads following single overload are studied by applying underloads in the step after overloads with OV/UN=1. Figures 5, 6, 7 show effect of underload following overload. In all three cases opening load values reduces due to underload. Maximum decrease in opening load value corresponding to OLR=1.67 with the value of 0.2 maximum load which is shown in Fig 9.

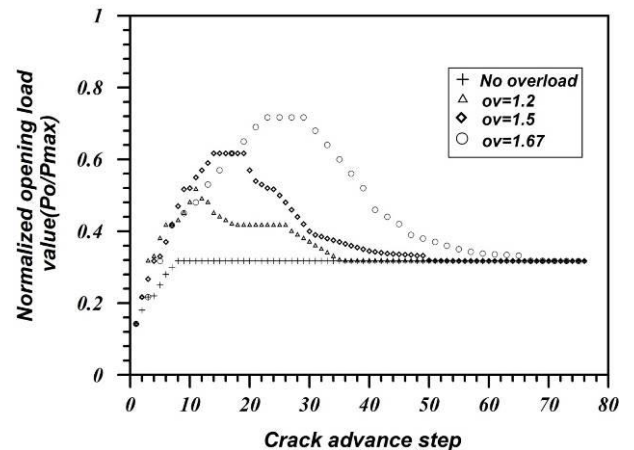


Fig 4. Effect of single overload on crack opening loads

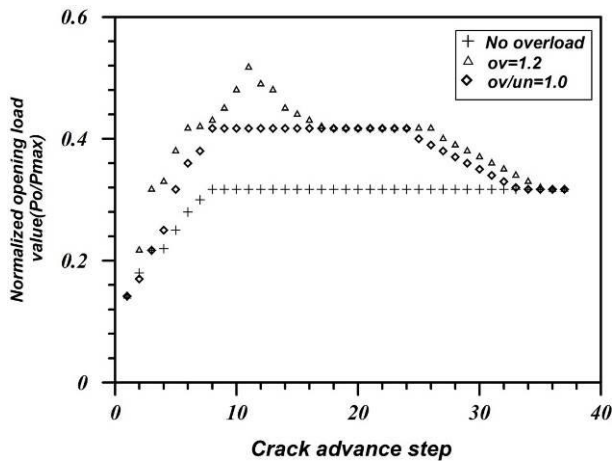


Fig 5. Effect of UN following single overload on crack opening value (OLR=1.2)

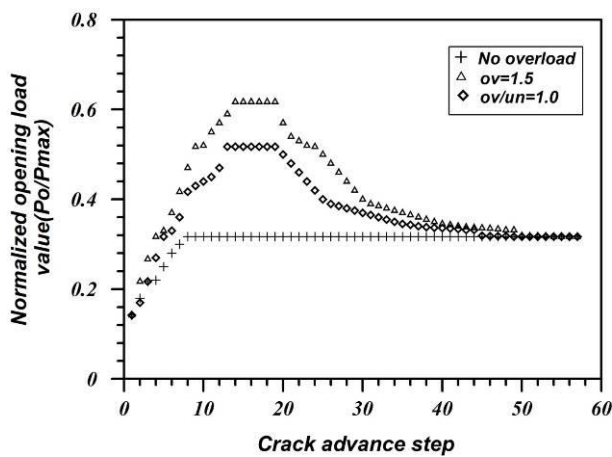


Fig 6. Effect of underload following by single overload on crack opening value (OLR=1.5)

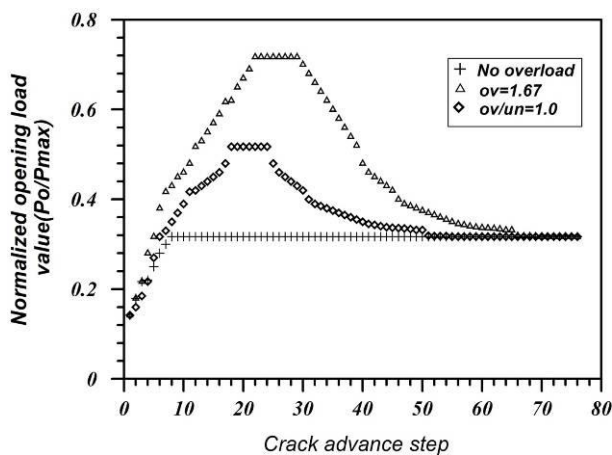


Fig 7. Effect of underload following single overload on crack opening value (OLR=1.67)

Finite element simulation of PICC indicates that overloads would result in higher opening load than no overload sequence. Higher opening load equals to lower stress intensity factor range which mean crack growth rate reduces due to overload. Higher OLR causes higher opening load and more reduction in crack growth rate. to prove this claim experimental results of Taheri's[5] researches are shown in table 4.

Table 4: Taheri's experimental results on 350WT steel crack growth subjected to several overloads [5]

| Case no | Overload ratio | Nf (experimental) |
|---------|----------------|-------------------|
| 1       | No overload    | 108000            |
| 2       | 1.2            | 130000            |
| 3       | 1.5            | 160000            |
| 4       | 1.67           | 219000            |

Table 5: Rushton's experimental results on 350WT steel crack growth subjected to underload [3]

| Case no | Overload ratio | OV/UN | Nf     |
|---------|----------------|-------|--------|
| 1       | No overload    | ----- | 108000 |
| 2       | OV=1.2         | 1     | 114301 |
| 3       | OV=1.5         | 1     | 119969 |
| 4       | OV=1.67        | 1     | 118132 |

Referring to table 4, Taheri's experiments indicate that higher OLRs cause higher crack growth retardation. These outcomes are in agreement with finite element simulation of PICC.

Moreover, pursue effect of UN on crack growth rates which studied by Rushton (table 5), illustrated that UN would decrease crack retardation effect of OV but it couldn't eliminate all the effects. Finite element simulation of underload following an overload has shown that crack opening load decrease as UN increases. Higher OLRs are much sensitive to underload and the crack retardation effect decreases.

## 6. SUMMARY AND CONCLUSION

Effects of a single overload, multiple overloads and an overload followed by a single underload on the center-cracked specimen of 350WT steel were investigated using finite element simulation of PICC. The following conclusions can be drawn from the analysis.

Single overload abruptly accelerates the crack growth immediately after overloading; however, crack retardation is the dominant effect following this acceleration period. Higher overload ratio results in higher crack growth retardation which leads to increase in fatigue life of the specimen. Underload would decrease the effect of overload but couldn't totally eliminate it.

## 7. REFERENCES

1. R.L. Carlson, G.A. Kardomateas and P.R. Bates, 1991, "the effects of overloads in fatigue crack growth", International Journal of Fatigue, 13:453-460.
2. S.Y. Lee, H. Choo, P.K. Liaw, et al. 2011, "A study on fatigue crack growth behavior subjected to a single tensile overload Part I. An overload-induced transient crack growth micro mechanism", Acta Materialia, 59:485-494.
3. P. A. Rushton, F. Taheri, 2003, "Prediction of crack growth in 350WTsteel subjected to constant

- amplitude with over- and under-loads using a modified wheeler approach”, *Marine Structures* 16:517–539.
4. D. S. Dawikie, 1997, “overload and underload effects on Fatigue crack growth behavior of 2024-T3 aluminum Alloy”, *Nasa contractor report*, 201668:1-9.
  5. F. Taheri, D. Traskb, N. Pegg, 2003, “Experimental and analytical investigation of fatigue characteristics of 350WT steel under constant and variable amplitude loadings”, *Marine Structures* 16: 69–91.
  6. Ch. Bichler, R. Pippan, 2007, “Effect of single overloads in ductile metals: A reconsideration”, *Engineering Fracture Mechanics*, 74: 1344–1359.
  7. G.A. Harmain, 2010, “A model for predicting the retardation effect following a single overload”, *Theoretical and Applied Fracture Mechanics*, 53: 80–88.
  8. A.U. de Koning, 1981, “A simple crack closure model for prediction of fatigue crack growth rates under variable-amplitude loading”, *Fracture Mechanics: 13th Conference, ASTM STP 743, American Society for Testing and Materials*, 63–85.
  9. J. Codrington, A. Kotousov, 2009, “Crack growth retardation following the application of an overload cycle using a strip-yield model”, *Engineering Fracture Mechanics*, 76:1667–1682.
  10. D. Nowell, 1998, “A boundary element model of plasticity-induced fatigue crack closure”, *Fatigue and Fracture Engineering Material and Structure*, 21: 857–71.
  11. W.Elber, 1970, “Fatigue Crack Closure under Cyclic Tension”, *Engineering Fracture Mechanics* 2:37-45.
  12. J.D Skinner, S.R. Daniewicz, 2001, “Simulation of Plasticity-induced Fatigue Crack Closure in Part-through Cracked Geometries using Finite Element Analysis”, *Engineering Fracture Mechanics* , 69 :1-11.
  13. J.E. LaRue, S.R. Daniewicz, 2007, “Predicting the Effect of Residual Stress on Fatigue Crack Growth, *International Journal of Fatigue*”, 29:508-515.
  14. K. Solanki, S.R. Daniewicz, J.C. Newman, 2004, “Finite Element Analysis of Plasticity-Induced Fatigue Crack Closure: an Overview, *Engineering Fracture Mechanics*”, 71:149–171.
  15. K. Solanki, S.R. Daniewicz, J.C. Newman, 2003, “Finite Element Modeling of Plasticity-Induced Crack Closure with Emphasis on Geometry and Mesh Refinement Effects”, *Engineering Fracture Mechanics*, 70:1475-1489.
  16. RC. McClung, H. Sehitoglu, 1989, “On the Finite Element Analysis of Fatigue Crack Closure—1. Basic Modeling Issues”, *Engineering Fracture Mechanics*, 33:237-252.
  17. J.Z. Zhang, P. Bowen, 1998, “On the Finite Element Simulation of Three-dimensional Semi-Circular Fatigue Crack growth and Closure”, *Engineering Fracture Mechanics*, 60:341- 360.
  18. P.F. De Matos, D. Nowel, 2007, “On the Accurate Assessment of Crack Opening and Closing Stresses in Plasticity-induced Fatigue Crack Closure Problems”, *Engineering Fracture Mechanics*, 74: 1579-1601.
  19. S. Ismonov, S.R. Daniewicz, 2010, “Simulation and Comparison of Several Crack Closure Assessment Methodologies using Three-dimensional Finite Element Analysis”, *International Journal of Fatigue*, 32:1322-1329.
  20. A. Castro, G.P. Potirniche, 2010, “Multi-mechanism crack closure simulations in various steels”, *International Journal of Fatigue*, 32:1764–1773.

## 8. NOMENCLATURE

| Symbol           | Meaning                             | Unit     |
|------------------|-------------------------------------|----------|
| a                | Crack length                        | mm       |
| E                | Elasticity modulus                  | Gpa      |
| $\sigma_y$       | Yield strength                      | Mpa      |
| $\sigma_{uts}$   | Ultimate stress                     | Mpa      |
| $\nu$            | Poisson ratio                       | ---      |
| dN               | Number of fatigue cycles            | ---      |
| da               | Increment of crack growth           | mm       |
| g(x)             | material crack growth function      | mm/cycle |
| r <sub>p</sub>   | Crack tip plastic zone radius       | mm       |
| L                | Minimum element length at crack tip | mm       |
| K <sub>max</sub> | Maximum stress intensity value      | Mpa√m    |
| K <sub>min</sub> | Minimum stress intensity value      | Mpa√m    |
| K <sub>op</sub>  | Opening stress intensity value      | Mpa√m    |
| $\Delta k_{eff}$ | Effective stress intensity range    | Mpa√m    |
| PICC             | Plasticity Induced Crack Closure    | ---      |
| OV               | Overload                            | ---      |
| OLR              | Overload Ratio                      | ---      |
| UN               | Underload                           | ---      |
| OV/UN            | Overload/ Underload ratio           | ---      |
| B.C              | Boundary Conditions                 | ---      |

## 9. MAILING ADDRESS

**M. H. Gozin**

K.N. Toosi University of Technology,

Tehran, Iran

E-mail: hgozin@dena.kntu.ac.ir